

Specialcourse Report
Master of Science in Electrical Engineering

DTU Space

National Space Institute

Feasibility Study for a Vision-Based Relative Positioning System for the UAV-QMS Project

Alejandro García-Vaquero Velasco
(s172926)

Kongens Lyngby 2018



DTU Space

National Space Institute: Geodesy

Technical University of Denmark

Electrovej

Building 328

2800 Kongens Lyngby, Denmark

Phone +45 45 25 97 69

www.space.dtu.dk

Abstract

The aim of this Specialcourse is to develop, test and improve an embedded system to relative position an attached bird with respect to a flying drone. This is achieved by a visual approach. It is part of the UAV-QMS project that has been active since 2013 and the final goal is to measure the geomagnetic field very accurately in order to map the crust minerals in the ground or detect mines in the soil or water.

The objectives are to test the robustness and accuracy of the vision algorithm, validate the architecture and test the payload box that will hold in place the system during the flight.

Preface

This specialcourse report was prepared at the department of Space at the Technical University of Denmark in fulfillment of the requirements for acquiring 10 ECTS as part of the MSc in Electrical Engineering.

Kongens Lyngby, May 23, 2018



Alejandro García-Vaquero Velasco (s172926)

Acknowledgements

This special-course would not have been possible with the tremendous effort and help given by Xiao Hu, Phd Candidate at DTU Space, which has helped me during the entire development of this course.

Additionally I want to thank Jakob Jakobsen and Daniel Haugård Olesen, both professors at the same department, to grant me the opportunity of working in this really interesting project and giving their time in order to supervise this special-course.

Contents

Abstract	i
Preface	iii
Acknowledgements	v
Contents	vii
1 Introduction	1
1.1 UAV-QMS Project	1
1.2 Relative Positioning System	2
1.3 Main Objective	2
2 Hardware Setup	3
2.1 Camera	3
2.2 Single Board Computer	5
2.3 Payload Box	5
3 Algorithm	7
3.1 Detection	7
3.2 Pose Estimation	8
3.3 Non-Linear Optimization	8
4 Experiments	9
4.1 Experiment #1	9
4.2 Experiment #2	15
4.3 Experiment #3	18
4.4 Experiment #4	22
4.5 Experiment #5	26
5 Conclusion	31
Bibliography	33

CHAPTER 1

Introduction

1.1 UAV-QMS Project

The objective of this project is to develop a multi-purpose, long range UAV for high Quality Magnetic Survey. Capable of being deployed anywhere, from ships to complex terrains, having a clean collection of data with minimal magnetic noise. Additionally it will bring a great reduction in cost compared to helicopter surveys.

This high resolution has many different applications:

- Exploration of natural resources
- Locating unexploded bombs

This would allow the plant of underwater cables for wind farms, usability of military tests sites or humanitarian projects.

The fundamental feature for magnetic survey is that measurements are close to the ground, or water, that would yield minimum noise levels and a precise position of such measurements. Nowadays, such surveys are done by helicopter with an attached magnetometer "bird". Heliborne surveys are very costly, challenging, slow and incomplete. So efficient exploration in remote places are hampered by existing methods.

This project will use as a flying platform the recently developed Smart UAV, a hybrid UAV with VTOL and hovering capabilities . Furthermore a bird will be hanging from some lines with a high resolution magnetometer attached. This will allow having some distance from the powerful electronics of the flying vehicle and avoid electromagnetic interference to have a cleaner data acquisition.

The first tests will focus in clearing the mines from WWII in order to place power lines for offshore wind farms. It will also be tested in the Greenland mountains to search for mineral deposits or military waste. In such both applications the VTOL capability is significant.

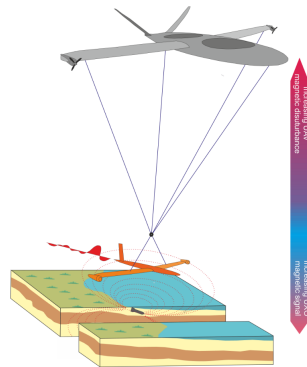


Figure 1.1: UAV-QMS Sketch.

1.2 Relative Positioning System

For this whole project to work it is of critical importance to localize relatively, from the Smart UAV to the bird, the position and orientation (pose) for the measurements to have a sensible meaning. There are several different approaches to solve this challenge but in this special-course the focus will be in the Vision-Based solution.

The main idea is to install a whole embedded system with a camera pointing downwards to the bird and with the help of some markers, using computer vision, extract the relative pose of the bird and match this pose with each of the magnetometer measurements.

1.3 Main Objective

The main objective of this special-course is to validate and proof the viability of the Visio-Based approach for the UAV-QMS project.

To do so there will be many benchmarks and robustness tests for the system as for example:

- Varying lighting conditions
- Marker size
- Marker distance
- Marker occlusion
- Camera model and configuration (model, exposure time, aperture, FPS, resolution)
- Response to vibrations

CHAPTER 2

Hardware Setup

In this section the Hardware used for the experiments and probably the final setup will be described.

2.1 Camera

2.1.1 Matrix Vision

2.1.1.1 Sensor

The sensor is 5.1 Megapixel (2464*2056) and has a global shutter with a maximum frame rate of 35.6Hz and a wide range of exposure time from 20 μ s to 1s. The sensor size is 2/3". It has both colour and greyscale capabilities and several options to trigger it. For this application the USB3.0 will be used along the SDK Matrix Vision provides.



Figure 2.1: Sensor Matrix Vision mvBlueFox3-2051a.

2.1.1.2 Lens

This lens has a fixed focal distance of 12.5mm, an Iris range of F1.4 to F22 and a manual focus. The major drawback of this lens is that weights 295g which is a great part of the weight for the positioning system.



Figure 2.2: Lens Fujinon HF12.5SA Focal Length 12.5mm fixed.

2.1.2 GoPro

The GoPro is a very interesting option as it is very low weight, has a great FOV and its own battery and capturing system. Also several capturing frequencies and resolutions are available from 30 to 120 FPS and 720p to 4K.



Figure 2.3: GoPro Hero 6 Black Edition.

2.2 Single Board Computer

2.2.1 Odroid

It is a low consumption Single Board Computer (SBC) with an ARM architecture, 2GB of RAM and 32GB of High Speed flash storage. In order to start the capturing and SSH connection is established by Ethernet, but it could be improved by using a WiFi module, and the capturing script is launched.

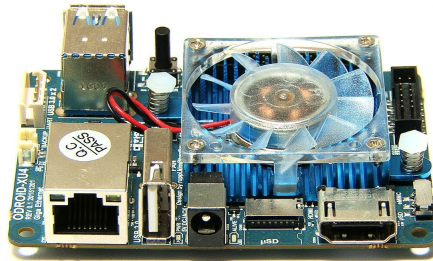


Figure 2.4: SBC Odroid XU4.

2.3 Payload Box

The Payload box where all the Hardware is mounted is based on a previous standardized design used for all the different research projects in the lab, as the drones have already a mounting system for these dimensions. It is made on laser-cut wood.

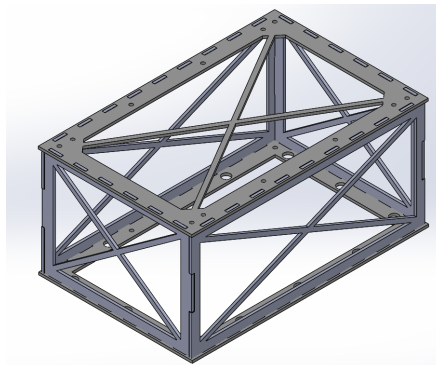


Figure 2.5: Payload Box.

CHAPTER 3

Algorithm

In this section the algorithm work-flow is briefly described to understand better the localization process.

The algorithm described is based on *WhyCon* [Kra+13] solution to develop a cost-effective, robust and accurate localization system. The algorithm has been refined and modified to suit better the final application.

3.1 Detection

In this section the first part of the algorithm will be described. The detection of the marker is the most important part as a robust and accurate detection of the circular crown will yield the best results.

The **outer** and **inner diameter** lengths are defined in the code in order to extract the position of the marker.

3.1.1 Threshold

The algorithm uses the grey-scale image. An **adaptative threshold** mean, with a 7x7 moving window, is applied and then an **inverted binary threshold**. This way it is ensured that the black crown of the marker is isolated in the image.

After having the binary image **erosion** is applied in order to remove small black regions that may have escaped the first thresholds.

3.1.2 Contour Detection & Ellipse Fitting

After the preprocessing some geometric and shape condition thresholds are manually defined, as the size of the contour, the roundness or the area ratio between the inner circle and the outer one.

After this there are two options, First image moments, up to second order, for the contour are calculated to infer the area, perimeter, orientation angle and minor and major vectors axes.

Secondly it is also possible to apply direct ellipse fitting where the contour is forced to satisfy an ellipse equation in the plane and so get the parameters from the equation.

After determining all the possible ellipse candidates a last filter is applied to remove false positives.

3.2 Pose Estimation

In this part there is a first estimation of the position of the marker relative to the camera. This is done by the use of the homography matrix that is extracted when you set the origin axes.

The 2D position of the ellipse is transformed to the 3D position relative to the camera using the parameters of the camera obtained by the camera calibration algorithm and so a first iteration for the position of the markers is calculated.

3.3 Non-Linear Optimization

After the first initial estimation of the position is calculated a non-linear optimization is executed on the set of points obtained, knowing the configuration of a set previously defined in the algorithm.

This known configuration consists of three markers in a right-angle triangle arrangement. This way an origin and the positive x and y axes are described. The inter-distance between markers is known and fed to the non-linear optimization so the position of the other markers can be finely tuned and get a much more accurate and robust result.

CHAPTER 4

Experiments

In this section the experiments made during the process of the special-course will be described.

4.1 Experiment #1

The main objective of this experiment is to find out the static accuracy of the relative positioning algorithm and test preemptively the factors that may decrease this accuracy as, different lighting conditions, vibrations, and geometric distribution over the image.

To measure the ground truth an A0 graph paper is printed and installed on the whiteboard to make easier and more reliable readings. The reference frame is set to the top left marker of the 4 markers that are together, x-axis positive horizontal right, y-axis positive vertical down. The position of each marker is defined at the centre of the circles.

The camera is positioned 5m away from the whiteboard in order to reproduce the distance to the bird.

Ground-truth Relative Position of Markers (in m)	
Top Left	(0.667, 0.08)
Top Right	(1.029, 0.017)
Bottom Left	(0.478, 0.612)
Bottom Right	(0.95, 0.482)

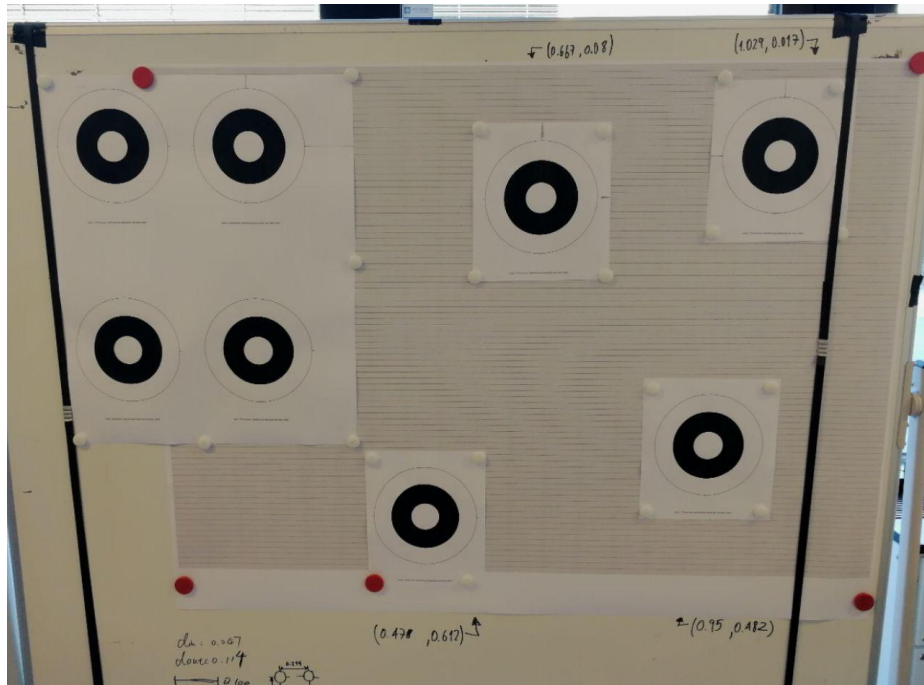


Figure 4.1: Experiment Setup with manually measured positions.

4.1.1 Test 1

In this first test the position accuracy is measured with the proposed algorithm.



Figure 4.2: Accuracy Test.

Measured Relative Position of Markers (in m)		
	Ground Truth	Measured
Top Left	(0.667, 0.08)	(0.66, 0.08)
Top Right	(1.029, 0.017)	(1.02, 0.02)
Bottom Left	(0.478, 0.612)	(0.48, 0.6)
Bottom Right	(0.95, 0.482)	(0.94, 0.47)

As it can be seen the accuracy is sufficient to determine the relative position within a 1cm error.

Also the detection of the markers is very robust as blocking a marker and then revealing it would not affect at all.

4.1.2 Test 2

In the second part of the experiment we tested the accuracy with a very basic human introduced vibration to the camera. See video uploaded to ownCloud.

With low amplitude vibrations the accuracy was the same as on static test.

With high amplitude vibrations the positions started changing as the camera was moving with respect to the whiteboard. The accuracy decreased to a 5cm error.

Additional test with more reliable vibrations should be taken whenever the Opti-Track is available.

4.1.3 Test 3

In the third part of the experiment several lighting conditions where tested. Firstly general exposure was tested with both underexposed and over exposed images.



Figure 4.3: Exposure Time $500\mu s$ (No reference frame).

In fig.4.3 the fourth marker to define the reference frame is not detected so the position estimates are not correct. This image is shown to show the capabilities of the ellipse detection under extreme low lighting conditions. The position information should **not** be taken into account.

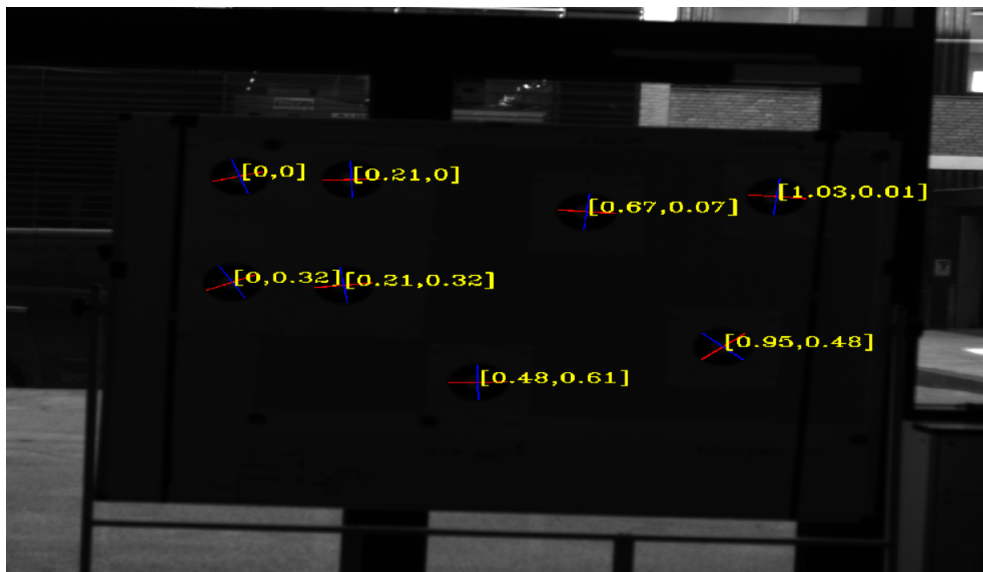


Figure 4.4: Exposure Time $1000\mu\text{s}$.

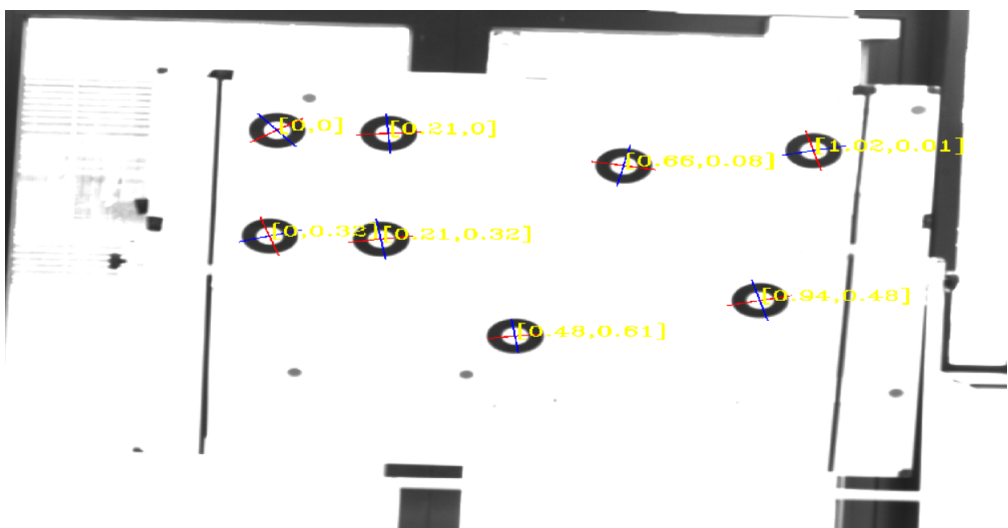


Figure 4.5: Exposure Time $50000\mu\text{s}$.

As it has been proven that the accuracy is not affected by different lighting conditions as the ellipse detection is very robust, positions in both $1000\mu\text{s}$ and $50000\mu\text{s}$ are the same.

An additional test was taken consisting on lighting just one of the markers with a LED flood-light, in order to have different intensity values for each marker, but no inaccuracies where noticed.

4.1.4 Test 4

In this last test the markers where placed in different corners of the image to test the camera calibration parameters and to test any distortion effects.

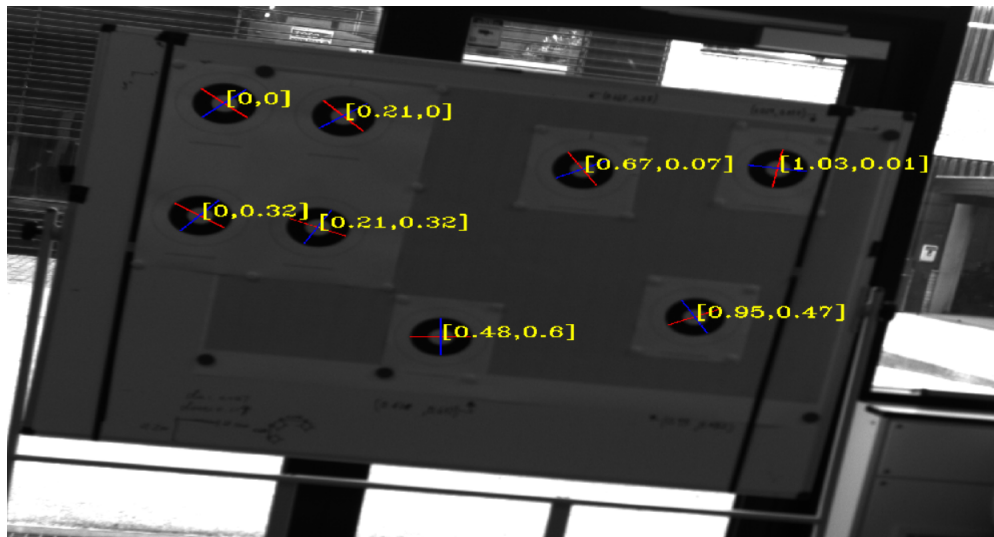


Figure 4.6: Top Right.

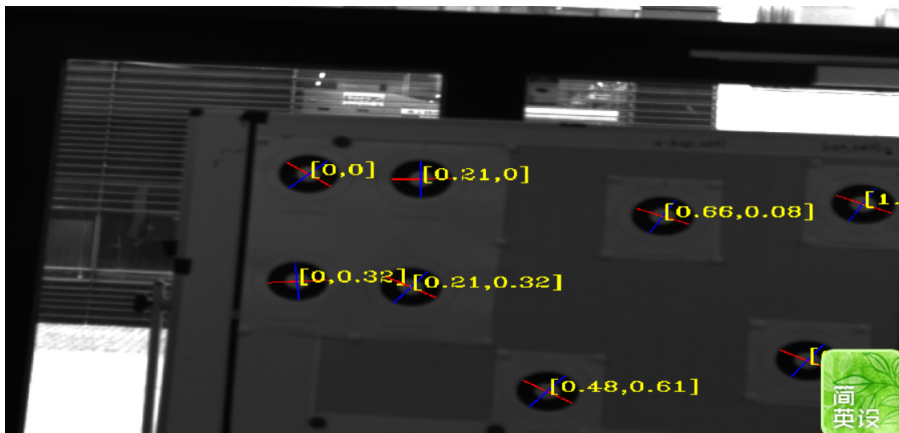


Figure 4.7: Bottom Left.

As it can be seen the relative position in both top right and bottom left are very similar.

4.1.5 Conclusion

The overall accuracy of the algorithm along the several tests is very robust, in all the tests the accuracy of 1cm was achieved.

- Further tests have to be developed once we have available the Opti-Track system for the ground-truth as it will be much more reliable and could test the error to mm scale.
- For the vibration test a solution has to be developed in order to introduce a known vibration (amplitude and frequency) to the system, although it has been proven there is not much motion blur and the detection is correct.
- The real flights will be over water so a more specific lighting experiment has to be developed in order to reproduce the possible reflexions and saturations from the water.
- It is advisable to get real flight data sets, even only with the hexa, in order to have a better base to test and fine-tune the algorithm.

4.2 Experiment #2

In this Experiment we test the accuracy of the positioning algorithm with respect to the depth distance of the camera to the markers.

Additionally we test 50% smaller markers in order to see the accuracy decrease

4.2.1 Test 1

In this part we test the algorithm accuracy from 3m to 8m distance to the markers.

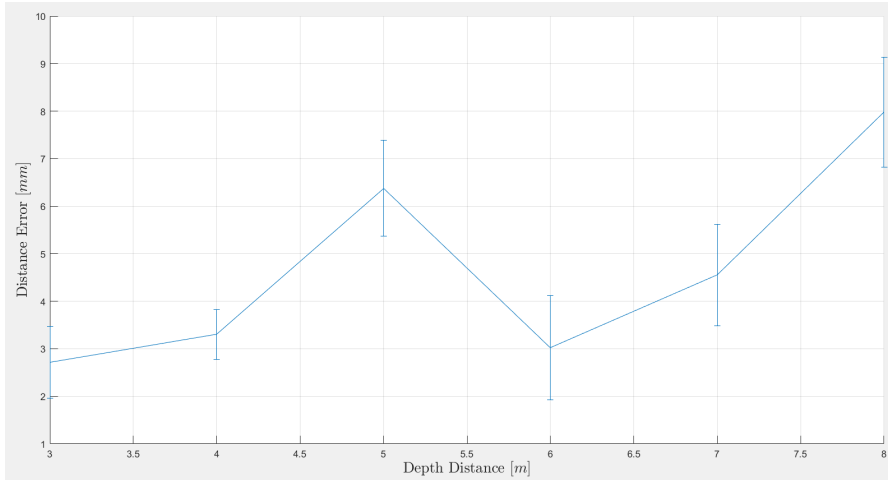


Figure 4.8: Absolute Position Error for several depths. .

As it can be seen the accuracy decreases when the distance increases but always remains smaller than 1cm.

Distance (m)	3	4	5	6	7	8
Mean Error (mm)	2.7153	3.3002	6.3751	3.0221	4.5508	7.9796
Std Dev (mm)	0.7520	0.5234	1.0103	1.0923	1.0628	1.1537

Table 4.1: Absolute Mean and Deviation Position Error for several depths..

4.2.2 Test 2

In this second test we test how the size of the marker can vary the accuracy. The markers used are a 50% smaller and both measurements are done at 5m distance.

Outer ϕ (mm)	114	56
Mean Error (mm)	6.3751	8.0440
Std Dev (mm)	1.0103	0.7722

Table 4.2: Mean and Deviation Error for 5m.

4.2.3 Conclusion

The accuracy is **below 1cm** in all the experiments so it can be validated for a static condition. The next test should be on a flying platform to see how the real vibrations affect the algorithm.

4.3 Experiment #3

In this Experiment we test the accuracy of the positioning algorithm using the OptiTrack system.

The setup for the experiment is the following. Attaching marker balls from the OptiTrack system to the camera and the marker and capture the position of both bodies with respect to the systems coordinate axes.

4.3.1 Test 1

In the first test the marker was moving continuously around the capturing volume and data was captured at 10Hz from the algorithm and 240Hz from the OptiTrack.

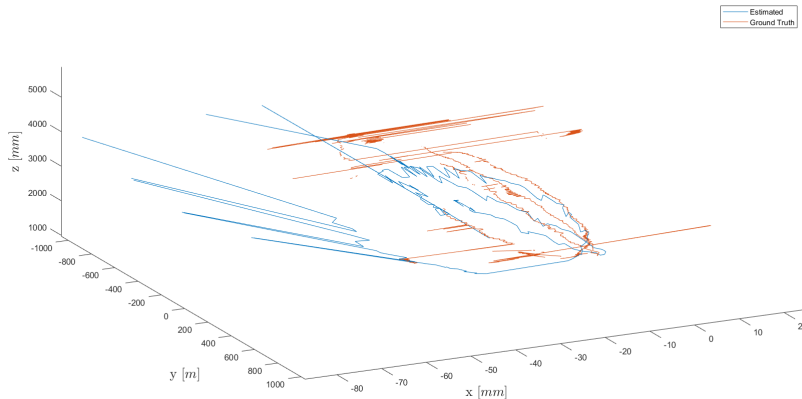


Figure 4.9: Test 1 Data. .

Analyzing the results from this test was extremely difficult as it was very hard to match the data. Also several systematic errors where made during this experiment. As the position or orientation offset of the data.

4.3.2 Test 2

In the second test we kept the marker static during several seconds in order to match both data easier. The position offset was solved satisfactory but the orientation error was very hard to eliminate.

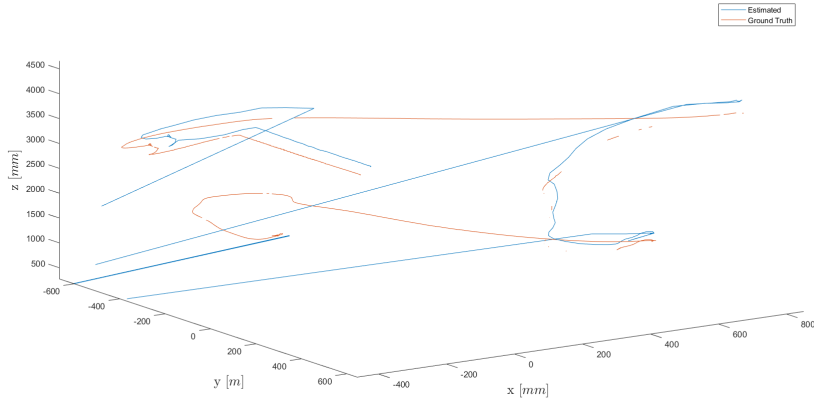


Figure 4.10: Test Data 2. .

4.3.3 Conclusion

During this experiment we faced several difficulties which reduced the quality of the results.

- Position offset from the OptiTrack rigid body and the actual center of the sensor or marker.
- Misalignment between the camera frame and the OptiTrack frame
- In the continuous experiment the difference on sampling frequencies.

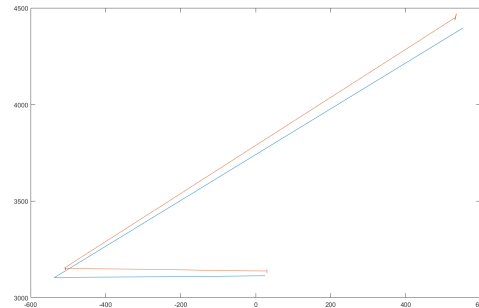


Figure 4.11: Ground Truth and Estimated Trajectories of the X and Y of the focused data. .

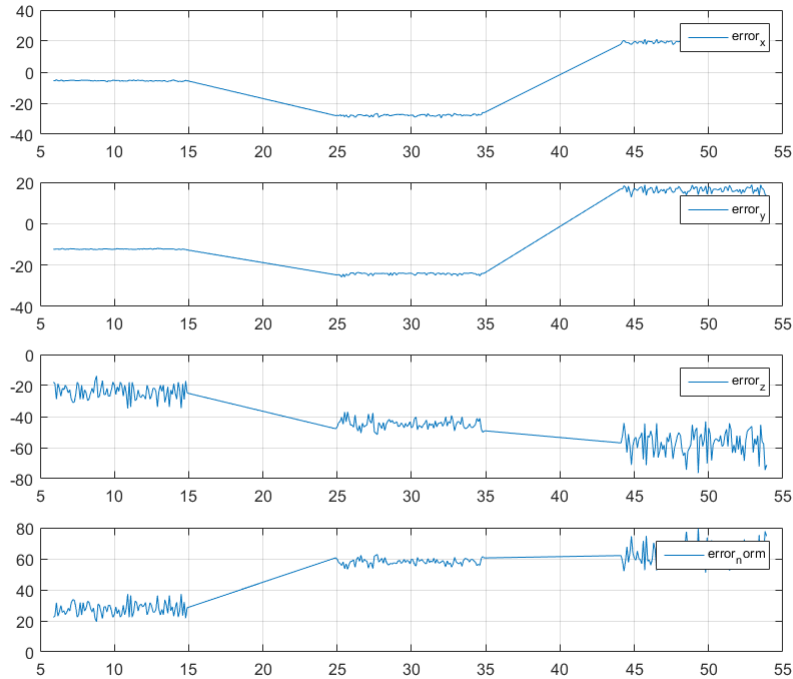


Figure 4.12: Position error in the different axis of the focused data... .

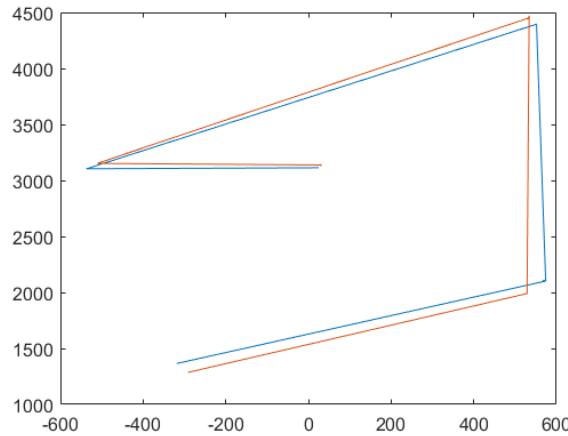


Figure 4.13: Ground Truth and Estimated Trajectories of the X and Y.

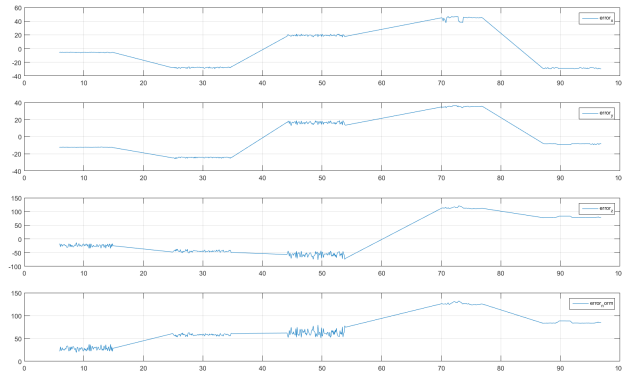


Figure 4.14: Position error in the different axis.

Analyzing the data several conclusions where extracted

- Calibration: when the marker is in the exterior part of the image the accuracy decreases significantly, showing there is a calibration error.
- Focus: The camera is originally setup for having the focus distance at 5m. The OptiTrack capture volume is not that big, so we are forced to do the experiment with depths around 3m, having a blurry image and affecting the accuracy.

4.4 Experiment #4

In this Experiment we test the accuracy of the positioning algorithm doing a real test flight. We use the payload box designed for the stereo odometry, removing one camera and orienting the other one to the ground.

We did a new calibration for the camera with the big chessboard in the lab at 5m in order to reduce error. We had to reduce the aperture in the camera in order to increase the depth field of the focus, but that made the exposure times increase and introduce a small image blurr.

Data capturing was done using the odroid at 10 FPS, working pretty decently with Xiao's adjustment in the capturing algorithm, as he improved parallel processing.

We printed a 4*2 Marker page in order to measure the relative position of each marker and do it in a accurate way in the flight tent. For the second and third test we added a marker on top of a box to add a relative depth measurement.

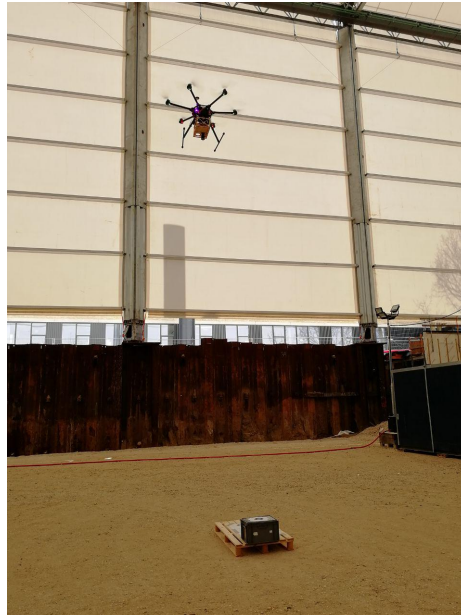


Figure 4.15: Experiment Setup.

4.4.1 Test 1

In the first test we only captured the printed page on the floor and calculated the 3D relative position of each of the markers with respect to one of them knowing the measured distance between them.

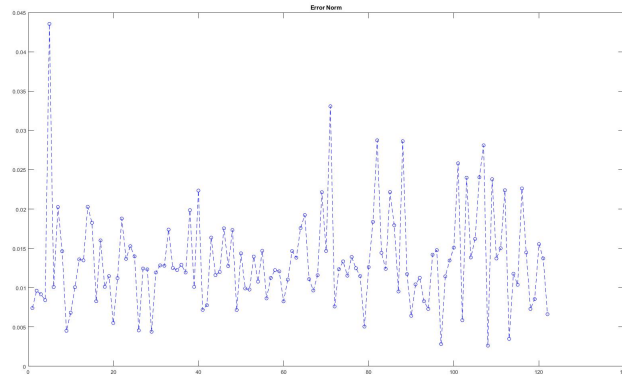


Figure 4.16: 3D Position Error of all of the markers in meters.

4.4.2 Test 2

In the second test a depth difference was added by using a box and measuring its relative position from the origin to capture the ground truth. We took two data sets in this configuration because in the first one there was a small occlusion of the box into one marker. In this test we only benchmarked the depth accuracy, as the algorithm had problems labeling each marker consistently.

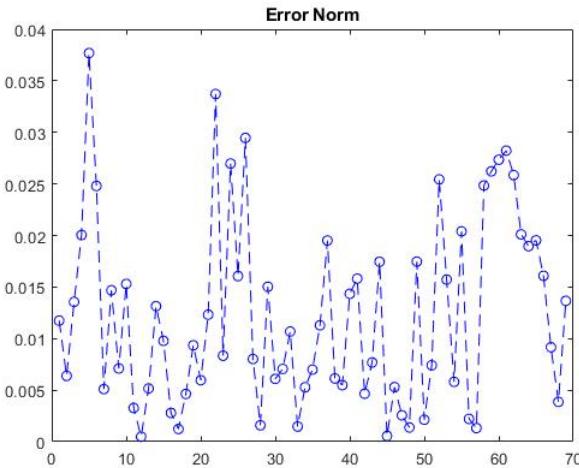


Figure 4.17: First Data Set with partial occlusion. Only depth error in metres.

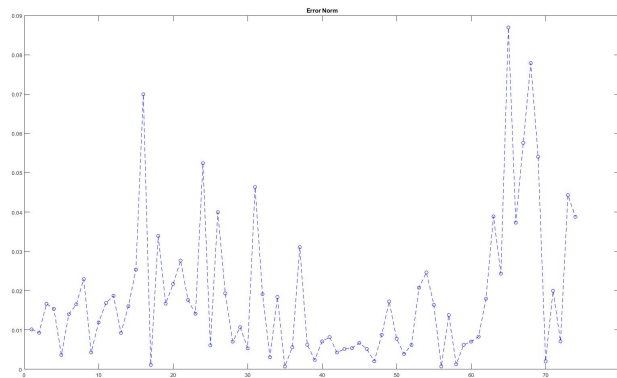


Figure 4.18: Second Data Set. Only depth error in metres .

4.4.3 Conclusion

The results from this experiment are very promising as there is nearly no error over 3cm. For the 3D position error it is consistent lower than 2cm and in the depth error the average is around 1cm.

The main problem with this experiment is that we calculate the relative distance of a marker relative to another marker in order to do some comparison with a ground

truth. We are not measuring the absolute distance from the camera to the marker as it is impossible right now to get this ground truth. It is possible there are some systematic errors that cannot get accounted using this benchmark system.

Also we encountered several problems with motion blurr. As we had to reduce the aperture in order to increase the depth of field, the exposure time had to be increased to have enough lighting in the image. This caused that when the drone was moving abruptly we had some missdetections from the algorithm or reduced the accuracy.

The flight test was succesfull for the embedded system as it proved reliable with the flying vibrations and other factors.

The next test will be trying out the GoPro camera as capturing system, if it proves reliable it can be an exceptional alternative as it is very cost-effective and also very light compared to the matrix camera + odroid configuration.

4.5 Experiment #5

This experiment was very similar to the previous one, but in this case we used the GoPro as a capturing device instead of the Matrix VISION Camera and Odroid setup. This would make a very interesting substitute as the GoPro is several times less heavy and the power consumption from the drone is nonexistent as it has its own battery.

The GoPro has several drawbacks as it has a very wide FOV for this application and an internal software preprocessing for the captured videos that may vary calibration and may not work for computer vision. Additionally it has a rolling shutter instead of the global shutter as the Matrix Vision.

4.5.1 Test 1

As in the previous test, we first do a simple test with all the markers printed in an A0 paper to ensure better accuracy for the ground truth

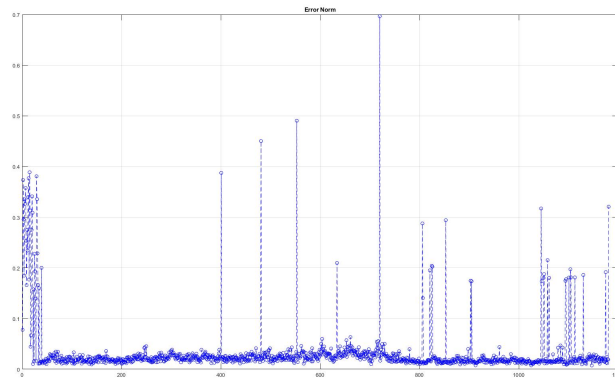


Figure 4.19: 2.7K 30FPS no Depth.

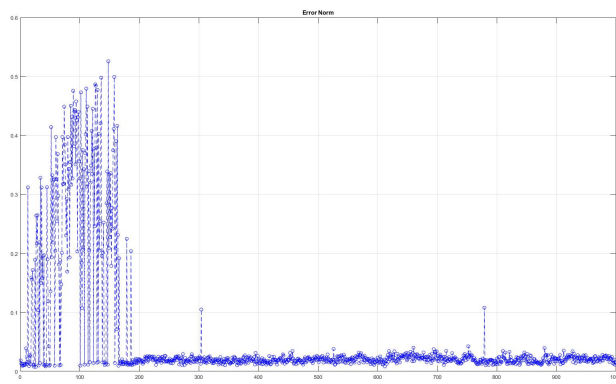


Figure 4.20: 2.7K 60FPS no Depth.

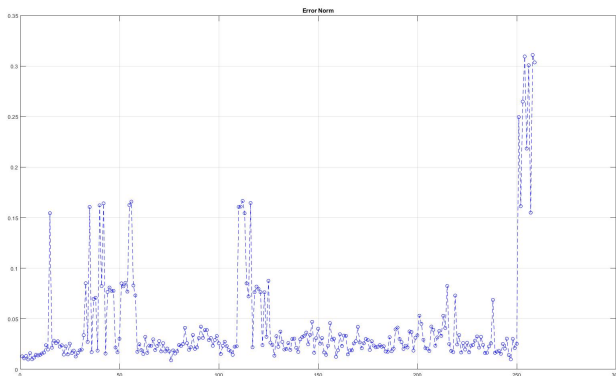


Figure 4.21: 1440p 30FPS no Depth.

In the next three plots a marker was added at a different height in order to asses depth accuracy too.

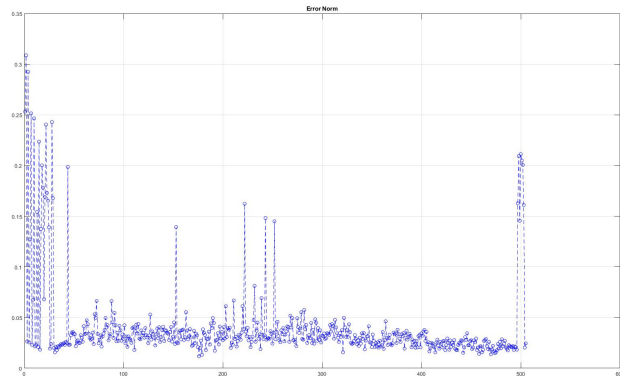


Figure 4.22: 1440p 30FPS Depth.

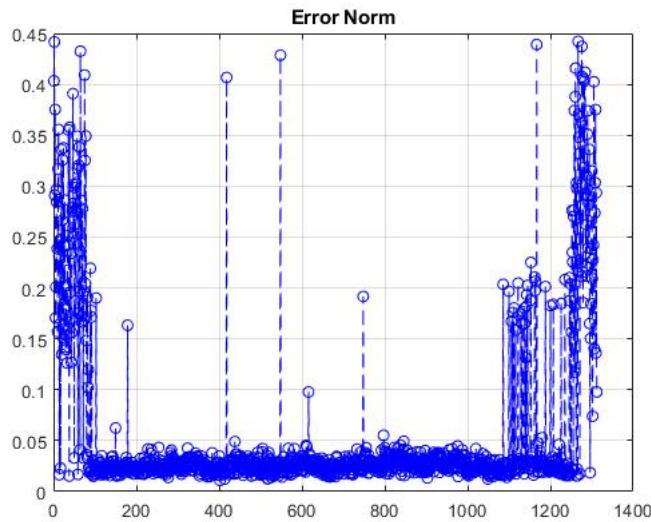


Figure 4.23: 2.7K 30FPS Depth.

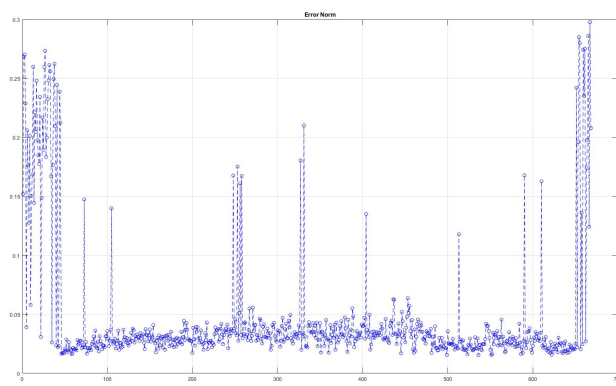


Figure 4.24: 1440p 30FPS Depth.

4.5.2 Conclusion

The results from the experiment were quite convincing even though we made some mistakes during the procedure, as having non-desired markers on the image or having the auto-stabilization feature activated on the camera, which would have affected the calibration of the camera, as the GoPro only captures a moving window crop from the full sensor and moves it in order to reduce blur and vibrations. This means that in different frames for the algorithm we would have the image from different parts of the lens and so different calibration parameters.

Table 4.3: Results from the benchmark.

Experiment	Mean 3D error (m)	Std Deviation	Outlier Filtering
2.7K 30FPS no Depth	0.0326	0.0558	none
2.7K 60FPS no Depth	0.0538	0.1001	none
1440p 30FPS no Depth	0.0434	0.0521	1σ
1440p 30FPS Depth	0.0400	0.0410	3σ
2.7K 30FPS Depth	0.0543	0.0818	3σ
1440p 30FPS Depth	0.0466	0.0546	3σ

As it can be seen the mean error is not over 6cm in any case which is very surprising as we believed it was going to be much bigger from the several factors commented previously.

As it can be seen at the beginning and ending of the plots there is a big increase in error due to the taking off and landing of the UAV, the markers where in the exterior part of the frame where the image suffers a great distortion due to the lens of the GoPro. Big peaks during the middle of the flight are due to misdetections of the algorithm.

CHAPTER 5

Conclusion

In this chapter the general conclusion for the vision based relative positioning system will be described.

The accuracy of the algorithm has been proven to be very reliable and robust. The system can deal with flight conditions as vibrations and rapidly changing lighting conditions do not affect the performance. Under several conditions the system proved to deliver an accuracy lower than 5cm in magnitude as shown in the experiments.

The aim of this special-course has been achieved and completed, the vision-based approach for the UAV-QMS project has been validated and the project can continue using this.

It is important to comment that the most crucial part of the configuration of the system is the length of the cord that carries the bird as this dimensions the size of the marker used in the bird and the size in pixels of the marker in the image. Changing this parameter would require to tune several parameters in the code. Additionally, it has to made sure that the lens used has a sufficient FOV in order to "see" the bird in every moment, even with strong side wind.

Bibliography

- [Kra+13] T. Krajník et al. “External localization system for mobile robotics”. In: *16th International Conference on Advanced Robotics (ICAR)*. November 2013. DOI: [10.1109/ICAR.2013.6766520](https://doi.org/10.1109/ICAR.2013.6766520).

